On the Variability of "Dynamic Seedability" as a Function of Time and Location over South Florida: Part I. Spatial Variability

WILLIAM R. COTTON[1] AND ALBERT BOULANGER

Experimental Meteorology Laboratory, NOAA, Coral Gables, Fla.

(Manuscript received 28 August 1974, in revised form 3 March 1975)

ABSTRACT

Using the one-dimensional cumulus model developed by Cotton, predictions of the effects of seeding cumulus clouds were performed during the month of July 1973 as a part of the Experimental Meteorology Laboratory FACE 1973 Experiment. The calculations were performed with the Miami 1200 GMT soundings and soundings taken in the interior of Florida at 1400 GMT at the so-called Central Site (CS) location.

A comparison of "seedability" predictions using the Miami 1200 GMT and CS 1400 GMT soundings have shown that substantial differences between the two seedability predictions occur on a number of days in spite of the fact that the soundings are separated in time by only 2 h and in space by only 110 km. The differences can be attributed to the frequent intrusion of dry air masses of varying height and thickness. The intensity of the dry layers is generally greatest over the higher-latitude CS location. The greatest differences between the two soundings, and hence the greatest difference between the predicted seeding effects, occurs during periods of transition from a disturbed, westerly flow regime to a well-defined, deep, easterly flow regime.

1. Introduction

It has often been the concern of meteorologists involved in the daily decision process of a weather modification experiment that the atmospheric sounding most readily available to the experimenter may not be representative of the actual sounding over the experimental area during the period of operation of the experiment. In the case of the Experimental Meteorology Laboratory (EML) cumulus modification experiments over south Florida, one of the main ingredients in the daily decision process has been the prediction of "dynamic seedability" using the National Hurricane Center Miami 1200 GMT sounding. The term "dynamic seedability" as used here is the same as that employed by Simpson and Wiggert (1969) where seedability represents the difference in predicted top heights between simulated seeded and unseeded clouds. The actual experiment is carried out approximately 100 km from the sounding site and often 5 to 9 h after the 1200 GMT sounding. During the course of the Florida Area Cumulus Experiment (FACE '73), we had the good fortune to have soundings observed within the center of the experimental area [the Central Site (CS)] at 1400, 1800, and occasionally at 2000 (all times GMT) from 4–31 July 1973 (see Fig. 1). The purpose of this paper is to examine the response of the one-dimensional entrainment model developed by Cotton (1972b); here called the PSU 71 model) to the 1200 and 1400 soundings mentioned above and to consider the impact of the associated "seedability" predictions on the daily decision process. In a subsequent investigation, we will analyze the temporal variability of "dynamic seedability" using the Miami 1200, CS 1400 and CS 1800 soundings.

2. Description of the "seedability model"

The model used for dynamic seedability calculations is the one-dimensional entrainment model developed by Cotton (1972b). Similar to Simpson and Wiggert (1969, 1971), seedability calculations are performed assuming that the lateral entrainment rate

$$\frac{1}{M}\frac{dM}{dZ}=\frac{0.18}{R} \tag{1}$$

is a constant for a given cloud tower radius (R). In addition, a virtual mass coefficient (γ) of 0.5 is employed and a precipitation fallout scheme similar to that of Simpson and Wiggert (1969) is used. The warm cloud microphysics is based on the work of Cotton (1972a) assuming that the initial cloud droplet concentration is 100 cm^{-3} and has a dispersion of 0.25. The mixed phase supercooled model is identical to that described by Cotton (1972b), with the condensed water substance divided among cloud droplets having a liquid water mixing ratio Q_c, raindrops assumed to be in a Marshall-Palmer spectrum having a mixing ratio Q_H, pristine and rimed ice crystals modeled in 21 discrete

[1] Present Affiliation: Department of Atmospheric Sciences, Colorado State University, Fort Collins.

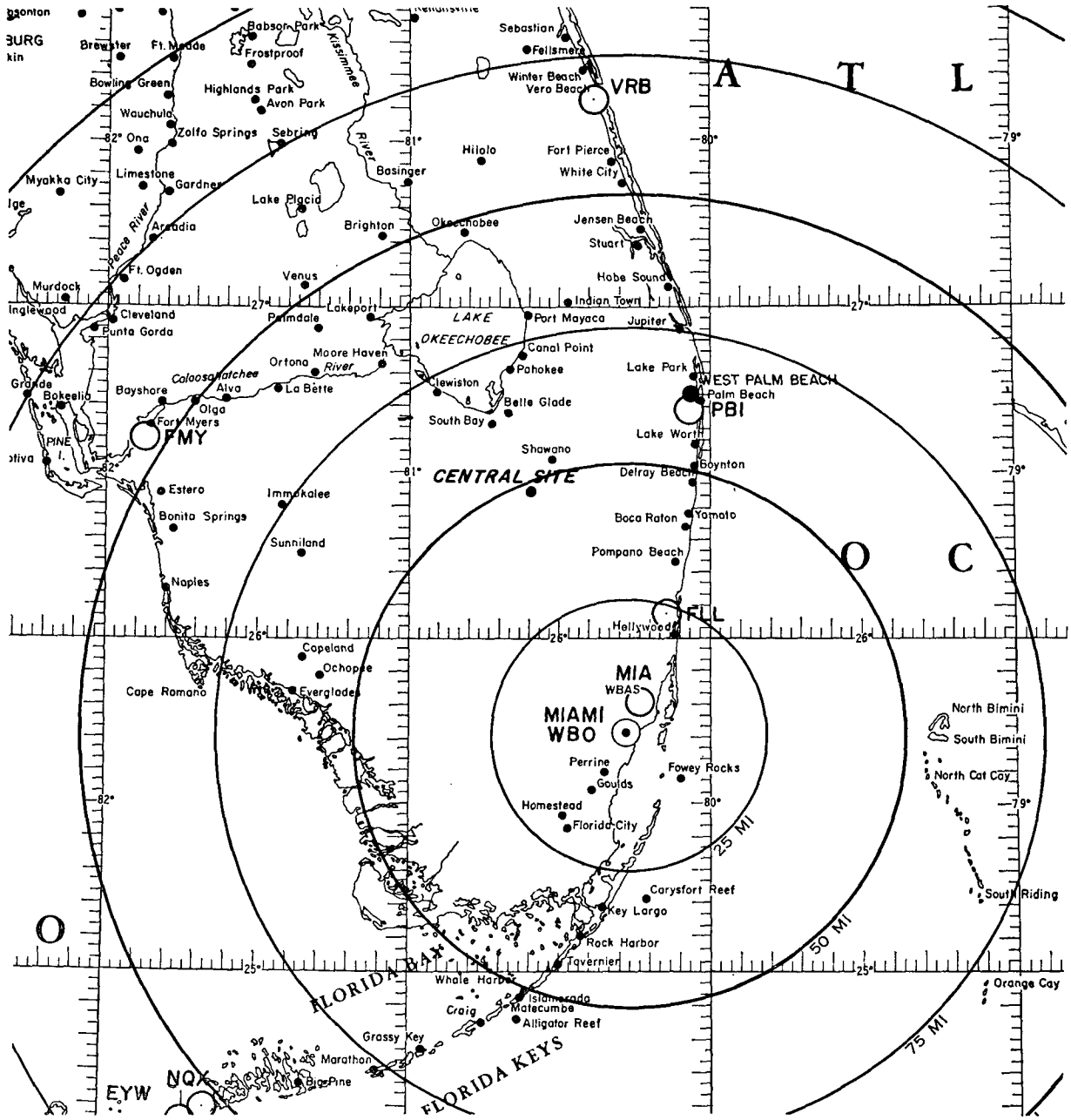

FIG. 1. Map of south Florida showing the location of the Miami and Central Site radiosonde stations.

categories whose combined mixing ratio is Q_I, and frozen supercooled rain assumed to be distributed in an inverse exponential distribution having a mixing ratio Q_F. Fig. 2 is a flow diagram illustrating the various microphysical processes modeled.

To simulate ice particle production, three models of ice crystal concentration as a function of temperature are hypothesized. The first assumes that the concentration of ice crystals formed in a cloud obeys the Fletcher (1962) exponential ice nuclei equation

$$N(T_s)=N_s e^{\beta_s T_s}, \quad (2)$$

where $N(T_s)$ represents the cumulative concentration of ice crystals nucleated at the degree of supercooling T_s, and β_s and N_s are assumed to be 0.6 and $10^{-5}\,\ell^{-1}$, respectively. Enhanced natural ice crystal production is modeled by multiplying (2) by the ratio of ice particles to ice nuclei as a function of temperature as suggested by Hobbs (1969). To simulate seeding, a cumulative crystal concentration of $5.5\times10^{4}\,\ell^{-1}$ is assumed to be nucleated between -4 and -7°C. This concentration was arbitrarily chosen in order to guarantee that the cloud model become glaciated at

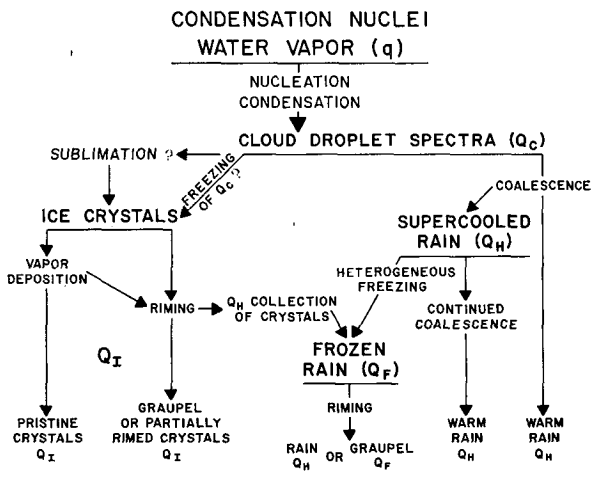

FIG. 2. Flow diagram of microphysical processes modeled in the seedability calculations.

temperatures warmer than −10°C under nearly all conditions experienced by the model. Fig. 3 illustrates the three ice particle production models. To compute seedability the two extreme ice particle production models are used. Thus, curve (a) in Fig. 3 is used for natural ice production and curve (c) represents the simulated seeded cloud ice particle production. Seedability in these numerical experiments is thus defined as the difference in predicted height between simulation (c) and simulation (a). As reported by Cotton and Boulanger (1975), the use of a natural ice production model simply lowers the amplitude of the seedability prediction but provides little additional information to be used for a daily decision process.

It should be pointed out that this seedability model differs in a number of ways from the EMB model reported by Simpson and Wiggert (1969, 1971). The microphysical processes in the supercooled portion of the EMB model are treated by direct analogy to the warm cloud auto-conversion-accretion parameterization scheme. A seeding subroutine is introduced by linearly freezing total condensate between the levels −4 and −8°C in the model. The latent heat of fusion is released and the cloud goes from water saturation to ice saturation in this interval. Natural glaciation is simulated either by releasing the latent heat of fusion linearly between −20 and −40°C or at −40°C. Orville and Hubbard's (1973) criticism of the arbitrary partitioning of the latent heat of fusion in the EMB model does not apply to the PSU 71 model. In the PSU 71 model cloud and rainwater are frozen according to the physical models of glaciation and freezing, and the cloud is isobarically adjusted to ice or water saturation at each integration step depending on the available cloud liquid water content.

Other differences between the two models have been reported by Simpson (1972). These are mainly related to the numerical procedure involved in performing the entrainment calculation. As pointed out by Cotton and Boulanger (1975), the combined effect of these differences results in a consistently higher seedability prediction by the EMB model than the PSU 71 model. In addition, the maximum seedability predicted on a given sounding by the PSU 71 model occurs at a smaller cloud radius than does the EMB model. As far as south Florida is concerned, there is no substantial difference between the two models as a decision aid. Of course, the decision maker must adjust his reference base for GO versus NO-GO accordingly. The main advantage of the PSU 71 model is that it is far more general and is adaptable to a broad range of input soundings at no additional computational cost.

3. Results of numerical experimentation

Seedability calculations were performed for the month of July 1973 using the Miami 1200 GMT sounding and the Central Site 1400 GMT sounding. Seedability was predicted for a spectrum of cloud radii of 0.5, 0.75, 1.0, 1.25, 1.5 and 2.0 km. The analysis was stratified according to whether the days were chosen as a GO day (actual randomized seeding experiments were performed), NO-GO day (the seedability was so poor or the radar coverage so large that the day was not suitable), or NO-Qualify day (the objective criteria suggested GO but observations in flight suggested the day was not suitable).

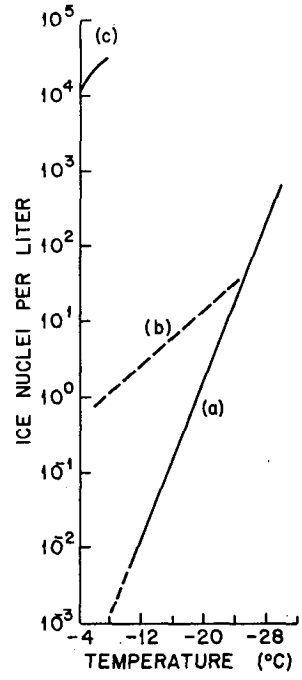

FIG. 3. Assumed ice crystal production as a function of temperature. Curve (a) represents natural ice particle production using the Fletcher (1962) nuclei spectrum, curve (b) an enhanced natural ice particle production, and curve (c) a seeded ice particle concentration.

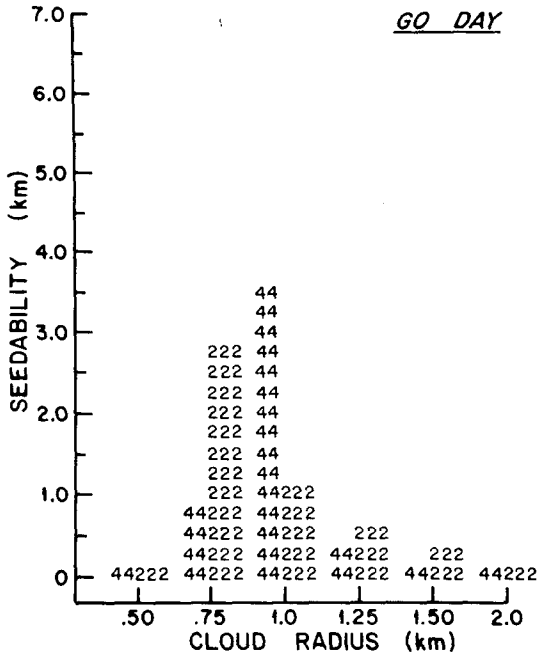

FIG. 4. An example of a predicted seedability spectrum for the MIA 1200 GMT sounding (222) and the CS 1400 GMT sounding (44) on a GO day.

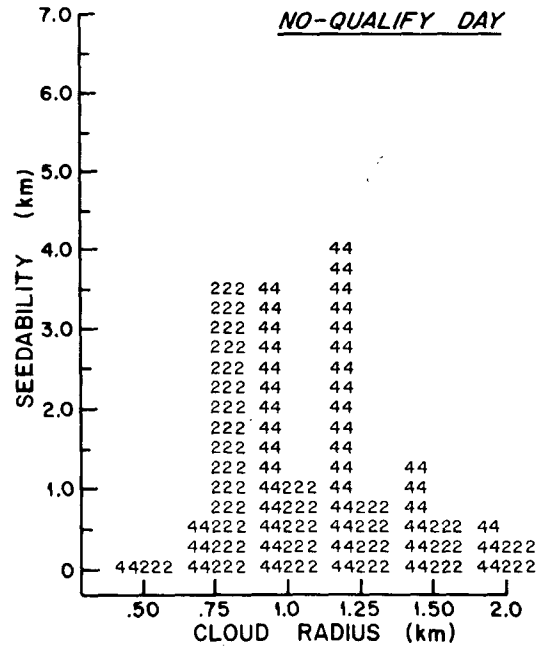

FIG. 5. An example of a predicted seedability spectrum for the MIA 1200 GMT sounding (222) and the CS 1400 GMT sounding (44) on a NO-Qualify day.

Fig. 4 is an example of a seedability spectrum for the 1200 GMT Miami (MIA) sounding and the 1400 GMT Central Site (CS) sounding. Using the MIA sounding, the model predicts a maximum seedability of 2.8 km at a cloud radius of 0.75 km. Using the CS sounding, on the other hand, the model predicts a maximum seedability of 3.5 km at a cloud radius of 1.0 km. Of the five GO days studied, two showed a shift of the radius at which maximum seedability occurred to larger radii and an increase of the magnitude of seedability with the CS sounding; two days showed no shift in the radius of maximum seedability with an increase in the magnitude of seedability with the CS sounding; the remaining day resulted in a bimodal seedability spectrum for the CS sounding, while the maximum predicted seedability occurred with the MIA sounding at an intermediate radius of 1.0 km.

Fig. 5 is an example of the seedability spectrum for a NO-Qualify day. The maximum predicted seedability occurred at a radius of 1.25 km with a magnitude of 4.0 km with the CS 1400 GMT sounding. With the MIA 1200 GMT sounding, the maximum seedability occurred at a smaller radius of 0.75 km and with a lower magnitude of 3.5 km. Three out of the five NO-Qualify days exhibited a similar shift of the seedability spectrum to larger radii and larger amplitude with the CS sounding. One day (24 July 1973) exhibited no shift in the radius of maximum seedability for a NO-Qualify day but a slightly larger amplitude for the MIA sounding was predicted. The fifth NO-Qualify day resulted in a peculiar seedability spectrum for both the MIA and CS soundings. As illustrated in Fig. 6 no seedability was predicted until a cloud radius of 1.25 km was prescribed, at which time the MIA sounding resulted in an abrupt increase in seedability amplitude. The CS sounding produced a similar behavior except

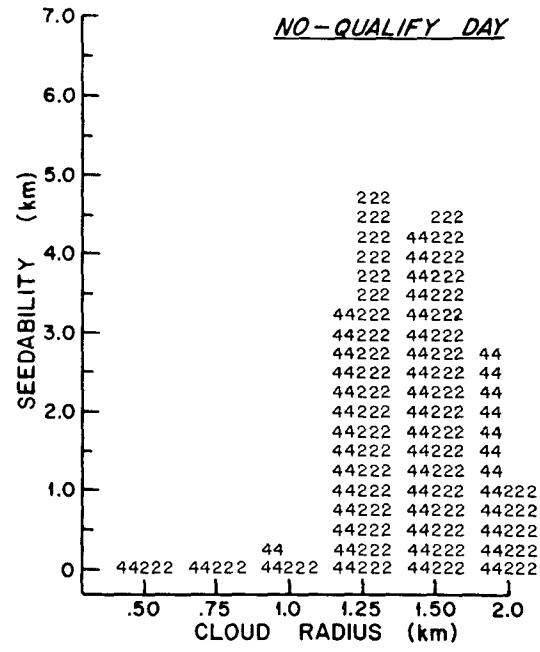

FIG. 6. An example of a peculiar seedability spectrum for the MIA 1200 GMT sounding (222) and the CS 1400 GMT sounding (44) on a NO-Qualify day.

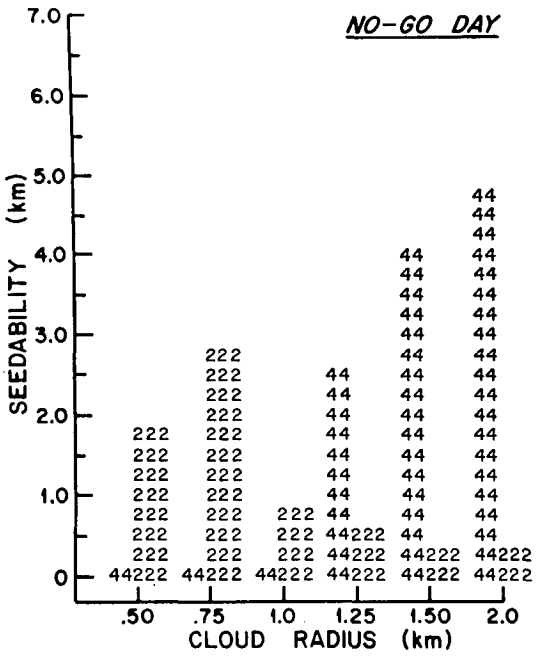

FIG. 7. An example of a shift of the seedability spectrum for the CS sounding (44) from the MIA sounding (222) on a NO-GO day.

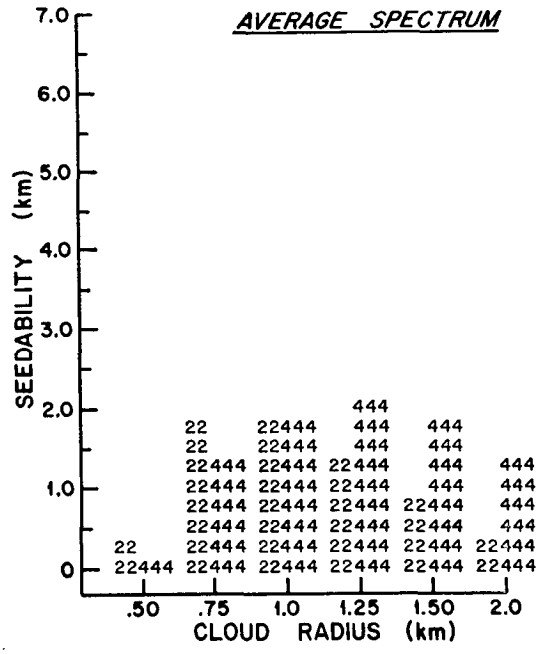

FIG. 9. Average seedability spectrum for the CS sounding (44) and MIA sounding (222).

that the rate of rise of seedability was slower, showing a maximum occurring at a radius of 1.5 km, but with a slightly lower amplitude than the MIA sounding.

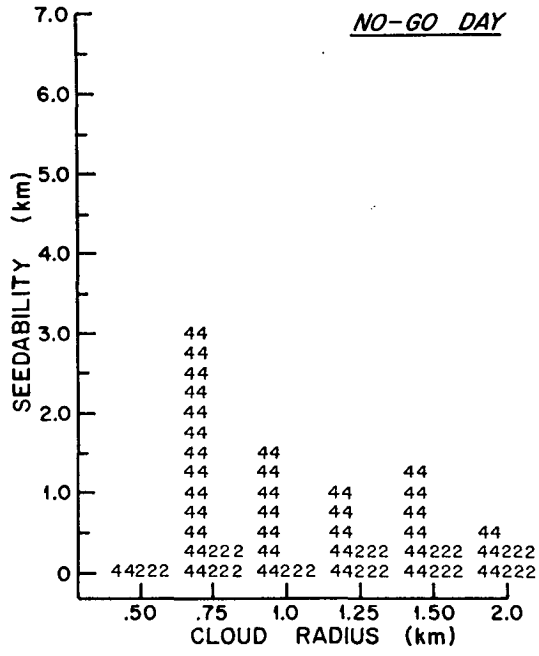

FIG. 8. An example of a significant predicted seedability on a NO-GO day using the CS sounding (44) with a negligible seedability predicted with the MIA soundings (222).

The greatest number of days (13 in all) analyzed fell in the NO-GO category. Of the thirteen days studied, six exhibited no significant difference between the seedability spectra for the MIA and CS soundings. Five of the thirteen days resulted in a substantial shift in the seedability spectrum to larger radii with the CS sounding. Fig. 7 illustrates such a spectral shift. On two NO-GO days, the seedability predicted with the CS sounding was significant, while that for the MIA sounding was negligible. Fig. 8 illustrates such a day. The true value of the Central Site soundings is best exhibited on NO-GO days which exhibited high predicted seedability at the Central Site with low values at Miami. There is little question that a NO-GO decision is the most reasonable decision based on the MIA seedability spectrum shown in Fig. 6, while the CS sounding may have resulted in a GO decision.

Combining the analysis of the seedability spectrum of GO, NO-Qualify and NO-GO days, we find an average seedability spectrum shown in Fig. 9. As expected, this illustrates that the CS 1400 GMT sounding results in a higher-amplitude maximum seedability and at a larger radius than does the MIA 1200 GMT sounding. The main reason for this behavior can be seen in Fig. 10 which shows the average Miami sounding and the average Central Site sounding for the days analyzed during July 1973. Except for the lowest levels below the assumed cloud base, the average temperature soundings at the two sites are virtually identical. The dew point soundings, on the other hand, indicate that the CS sounding is consistently drier than the MIA sounding.

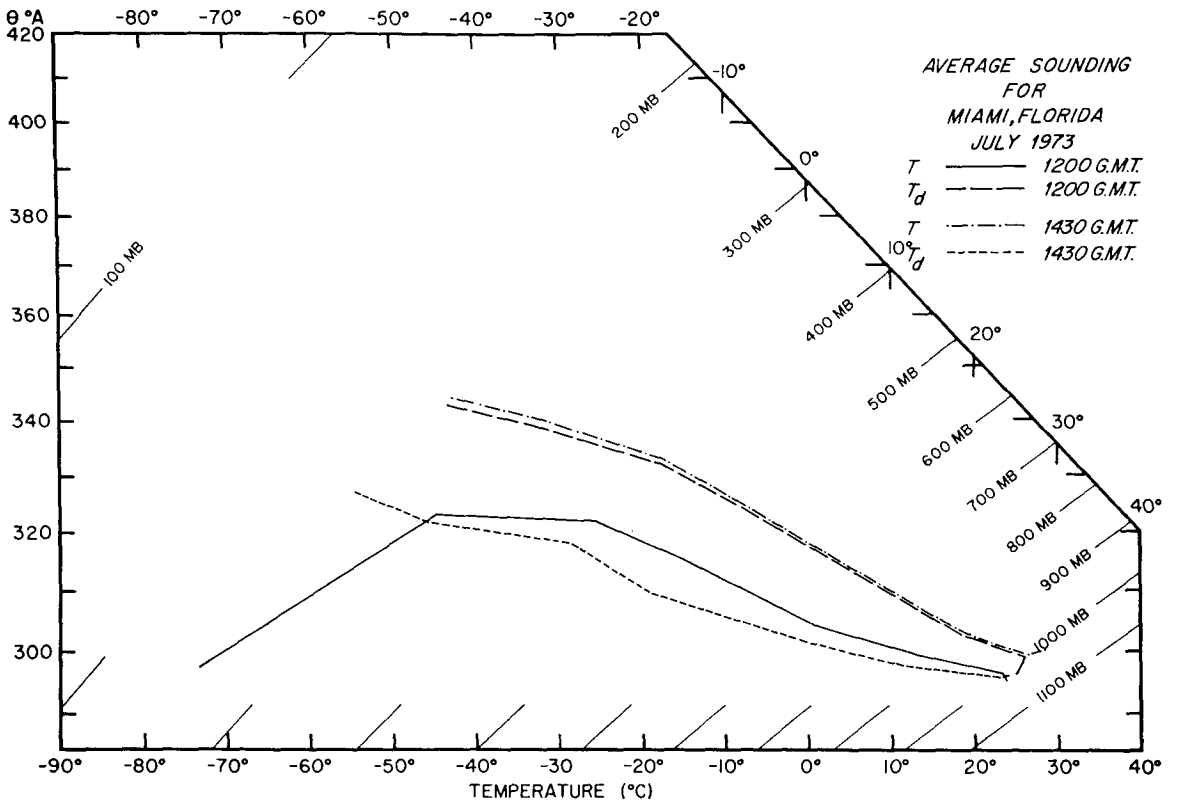

FIG. 10. Average Miami and Central Site soundings.

The response of the seedability model is such that smaller cumuli (radii < 1.0 km) are suppressed by the drier CS sounding, resulting in a lower seedability than the MIA sounding. Larger clouds (1.25 km radius), on the other hand, penetrate sufficiently deep into the atmosphere to allow effective activation of the seeding subroutine and result in an increased seedability for the CS sounding. Clouds of the same size in the higher moisture content MIA sounding penetrate so deep into the atmosphere that the natural nucleation model results in substantial natural glaciation and consequently lower seedability than the CS sounding.

We must now ask, "What is the reason for the drier average sounding over the Central Site?" Because the average CS 1400 GMT sounding is drier than the MIA 1200 GMT sounding throughout the depth of the sounding, one's first response is that the differences may be attributed to moisture sensor bias as opposed to a meteorological explanation. This would indeed be a disappointing conclusion.

An analysis of the individual soundings throughout the month of July 1973 indicates that the CS soundings are not consistently drier than the MIA soundings throughout the depth of the atmosphere on any individual day. Instead, while the temperature profiles at Miami and the Central Site may be nearly the same, a number of Central Site soundings exhibit intense dry layers of varying height, depth and intensity. While traces of such dry layers exist in the Miami soundings, their intensity is typically less. The 24 July 1973 soundings for Miami and Central Site, illustrated in Fig. 11, exemplify such a dry layer from 700 to 520 mb. Another dry layer above 400 mb at the Central Site and above 360 mb at Miami also can be seen in Fig. 11. The existence of the higher dry layer is quite common at both sites, but the CS sounding normally places the base of the dry layer at a lower altitude than does the MIA sounding. Because the dry layers are of varying depth and height, the result of averaging the sounding throughout the month is to "smear" the dry layers throughout the depth of the average sounding. The fact that the average CS sounding is consistently drier indicates that the intensity of the dry layer in the CS sounding is consistently greater than the MIA sounding.

Although the dry layers illustrated in Fig. 11 are associated with stable layers in the temperature profiles, the intensity and depth of the stable layers are so small that they are completely "wiped out" in the average sounding. Nonetheless, the existence of such a stable layer may, by itself or in combination with the dry layer, prevent the vertical development of clouds of a given size. This result also points out the obvious nonrepresentation of an individual sounding by an average sounding for use in convective model simulation.

The final question that must be answered is, "What is the source of the consistent difference in atmospheric

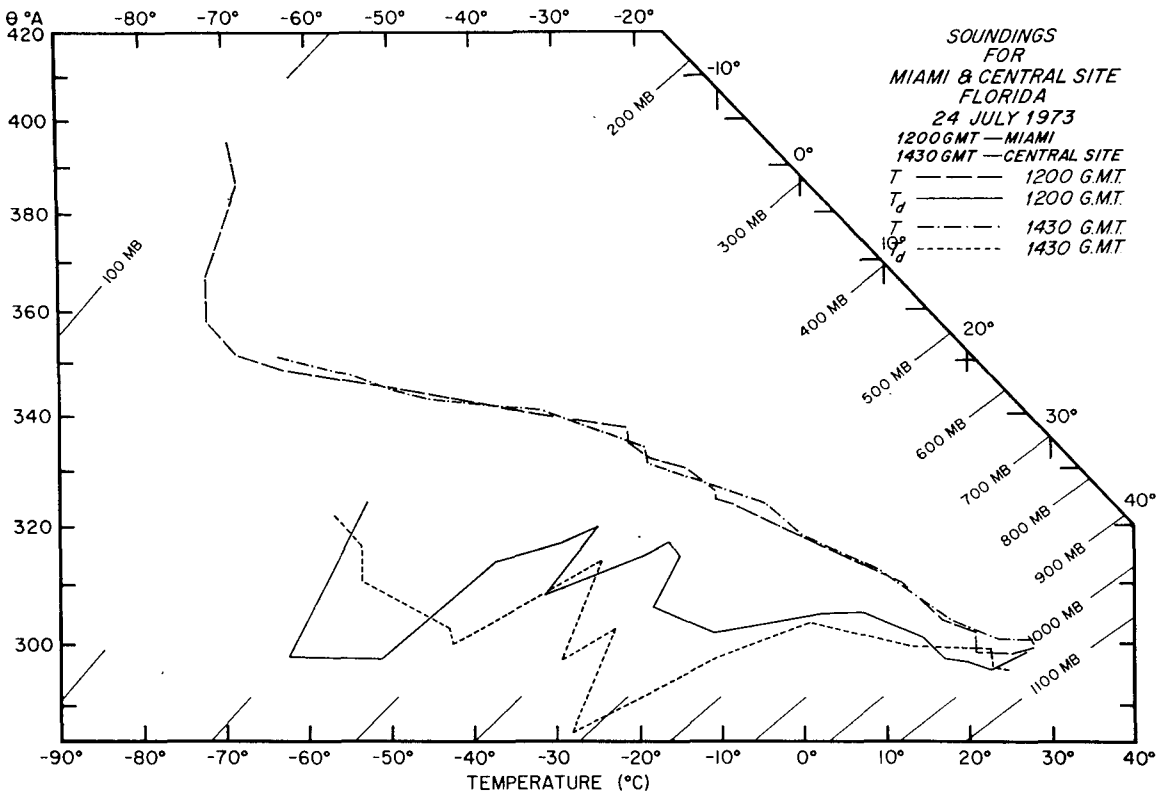

FIG. 11. 24 July 1973 CS 1400 GMT and MIA 1200 GMT soundings.

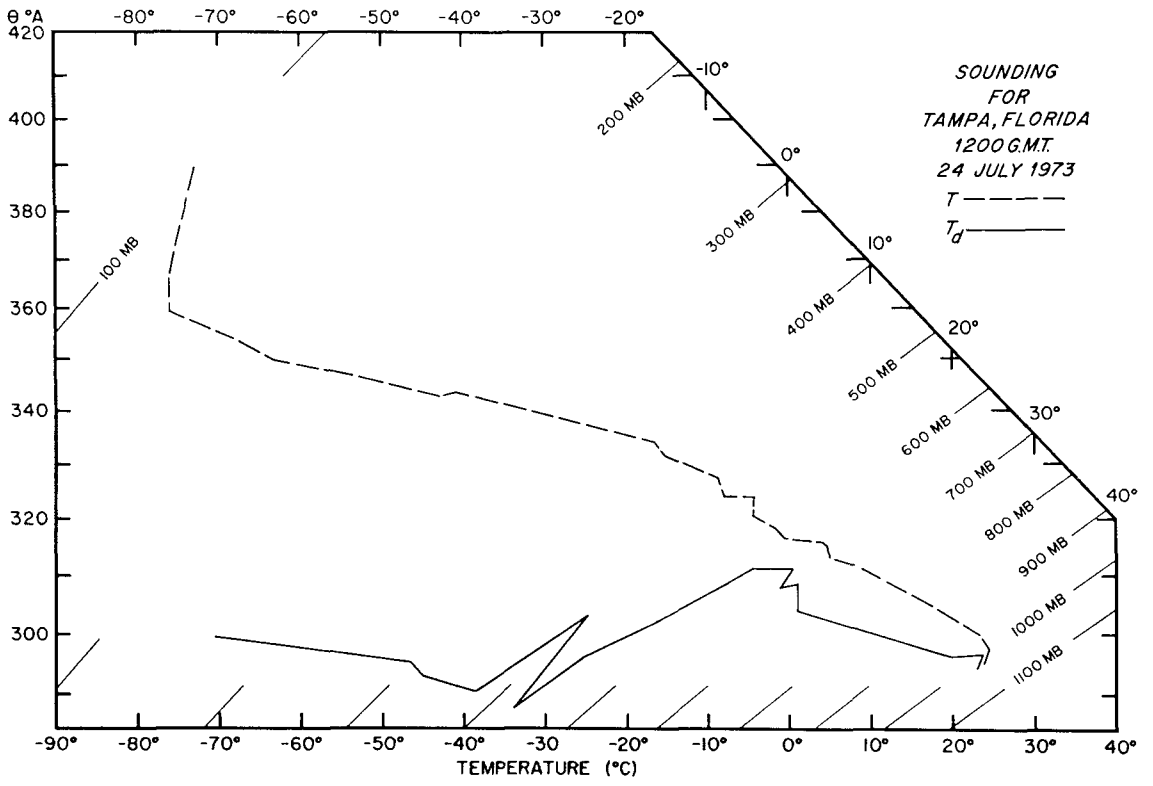

FIG. 12. 24 July 1973 Tampa 1200 GMT sounding.

soundings between Miami and the Central Site over a time span of only 2 h and a distance of only 110 km?" One possibility is that the differences are due to organized mesoscale disturbances. Because the thermal modification of the sounding is very shallow and both soundings are taken well before the onset of local deep convection, the likelihood that a mesoscale system might modify the air masses through the depth of the sounding is remote. Instead, the most probable source of sounding modification is a result of synoptic-scale influences. Support for this conclusion can be seen in the 1200 GMT 24 July 1973 Tampa sounding (110 km north of Sarasota in Fig. 1) shown in Fig. 12, where a pronounced dry air mass exists above 600 mb. It appears that the major differences between the CS and the MIA soundings occur during periods of transition from a disturbed, westerly-flow regime to a well-defined, deep easterly flow regime. Thus, the traditional view of the south Florida air mass during the month of July as a spatially and temporally deep easterly, homogeneous air mass was certainly not represented during July 1973.

4. Summary and conclusions

A comparison of seedability predictions using MIA 1200 GMT soundings and 1400 GMT soundings observed over the Central Site of the EML experimental target area during July 1973 have shown that substantial differences between the two seedability predictions occur on a number of days. This is in spite of the fact that the soundings are separated in time by only 2 h and in space by only 110 km. The differences are large enough to produce an average seedability spectrum over the Central Site which has a larger magnitude maximum seedability and occurs at a substantially larger cloud radius.

The differences in seedability predictions between the CS and MIA soundings can be attributed to the frequent intrusion of dry air masses of varying height and thickness. The intensity of the dry layers is generally greatest over the higher latitude Central Site location. The greatest differences between the two soundings, and, hence the seedability estimates, occur during the transition period from a disturbed westerly flow regime to a well-defined, deep easterly flow regime.

In agreement with Sax (1972) and in disagreement with Weinstein (1972), spatial variability in sounding data can, indeed, affect the climatology of dynamic seedability at least over a period of one month. Considering that this conclusion has been drawn from the analysis of data taken over south Florida during the month of July, which is traditionally viewed as a period being representative of a spatially homogeneous air mass, this conclusion is quite startling. In a central continental region, which is frequented by westerly disturbances, one would expect that spatial variability of sounding data would have an even greater impact on the climatology of dynamic seedability.

Acknowledgments. The authors wish to thank Dr. Robert Sax and Dr. William Woodley for their critical reading of the manuscript and encouragement to perform the above analysis. Ms. Polly Reyna typed the manuscript and Mr. Robert Powell drafted the figures. The numerical calculations were performed on the NOAA/MIAMI U1108 system.

REFERENCES

Cotton, W. R., 1972a: Numerical simulation of precipitation development in supercooled cumuli—Part I. *Mon. Wea. Rev.*, **100**, 757–763.

——, 1972b: Numerical simulation of precipitation development in supercooled cumuli—Part II. *Mon. Wea. Rev.*, **100**, 764–784.

——, and A. Boulanger, 1975: A comparison of "dynamic seedability" prediction with two cloud models during FACE '73. NOAA Tech. Memo. (in press.) [Available upon request to U. S. Dept. of Commerce, NOAA, Environmental Research Laboratories, Office of Director, Boulder, Colo.]

Fletcher, N. H., 1962: *The Physics of Rain Clouds*. Cambridge University Press, 386 pp.

Hobbs, P. V., 1969: Ice multiplication in clouds. *J. Atmos. Sci.*, **26**, 315–318.

Orville, H. D., and K. Hubbard, 1973: On the freezing of liquid water on a cloud. *J. Appl. Meteor.*, **12**, 671–676.

Sax, R. I., 1972: Comments on "Ice-phase seeding potential for cumulus cloud modification in the western United States." *J. Appl. Meteor.*, **11**, 1017–1018.

Simpson, J., 1972: Reply (to Jack Warner). *J. Atmos. Sci.*, **29**, 220–225.

——, and V. Wiggert, 1969: Models of precipitating cumulus towers. *Mon. Wea. Rev.*, **97**, 471–489.

——, and ——, 1971: Florida cumulus seeding experiment: Numerical model results. *Mon. Wea. Rev.*, **99**, 87–118.

Weinstein, A., 1972: Reply (to Robert Sax). *J. Appl. Meteor.*, **11**, 1018.